

Note

Effect of particle size of dry powder mannitol on the lung deposition in healthy volunteers

William Glover^a, Hak-Kim Chan^{a,*}, Stefan Eberl^b,
Evangelia Daviskas^c, Jordan Verschuer^b

^a Advanced Drug Delivery Group, Faculty of Pharmacy, The University of Sydney, NSW 2006, Australia

^b Department of PET and Nuclear Medicine, Royal Prince Alfred Hospital, Sydney, NSW, Australia

^c Respiratory Medicine, Royal Prince Alfred Hospital, Sydney, NSW, Australia

Received 1 May 2007; received in revised form 20 July 2007; accepted 7 August 2007

Available online 19 August 2007

Abstract

There is a lack of *in vivo* studies focusing on the effect of particle size of dry powder aerosols on lung deposition and distribution. We investigated the dose and distribution of radiolabelled powder aerosols of mannitol in the lungs using single photon emission tomography (SPECT). Three different sized radiolabelled powders were produced by co-spray drying mannitol with ^{99m}Tc-DTPA. The primary particle size distribution of the powders measured by laser diffraction showed a volume median diameter of 2, 3 and 4 μm with span 2.3, 2.0 and 2.1, respectively, which corresponded to an aerodynamic diameter of 2.7, 3.6, 5.4 μm and geometric standard deviation of 2.6, 2.4 and 2.7 when the powders were dispersed using an Aeroliser[®] dry powder inhaler. Three capsules each containing approximately 20 mg (i.e. a total of 60 mg containing 60–90 MBq) of each of the radiolabelled powders were inhaled by eight healthy volunteers using the Aeroliser[®] inhaler. Images of aerosol deposition in the lungs were acquired using fast, multi-bed position SPECT. The lung dose markedly decreased with increasing aerosol particle size (mean ± S.E.M.: 44.8 ± 2.4, 38.9 ± 0.9, 20.6 ± 1.6% for 2.7, 3.6, 5.4 μm, respectively, $p < 0.0001$). The sites of deposition of the 2.7 and 3.6 μm aerosols were similar (penetration index, PI = 0.63 ± 0.05, 0.60 ± 0.03, respectively, $p > 0.3$), but different to the 5.4 μm aerosols (PI = 0.52 ± 0.04, $p < 0.02$). The lung dose followed the *in vitro* powder dispersion performance, with the % lung dose being related to fine particle fraction by a slope of 0.8 for a regression with intercepts forced through the origin. The SPECT results provide direct evidence that the lung deposition of dry powder aerosols depends on the particle size. The lung dose of the 2.7 and 3.6 μm aerosols using the Aeroliser[®] was double compared to that of the 5.4 μm aerosols and the deposition of the smaller particles was more peripheral.

© 2007 Published by Elsevier B.V.

Keywords: Aerosol deposition; Particle size; Dry powder inhaler; SPECT imaging; Mannitol

1. Introduction

Particle size is an important determinant of *in vitro* aerosol performance for dry powder aerosols (Louey et al., 2004). Studies using mannitol and disodium cromoglycate have shown that as the particle size of powders is decreased, the fine particle fraction (FPF, i.e. % mass of particles < 5 μm in the aerosol) measured by cascade impaction is increased (Chew and Chan, 1999; Chew et al., 2000). While particles of small size are expected to be more difficult to disperse into aerosols due to increased cohesion (Zimon, 1969), increasing the inhaler dispersion efficiency

and air flow improves deagglomeration, leading to a larger FPF (Chew et al., 2000). Particle size is also known to affect deposition of dry powder aerosols in the lungs as well as therapeutic response (Zanen et al., 1994, 1995).

There have been many *in vivo* deposition studies using dry powder inhalers (DPIs). The focus of these studies has been on comparing DPI performance at different air flow rates (Newman et al., 1994; Meyer et al., 2004) or comparison with other DPIs, or with metered dose inhalers or nebulisers (Thorsson et al., 1998; Ball et al., 2002; Rohatagi et al., 2004). Most studies have used commercial DPI products where the particle size distributions of the powders were already fixed. Few studies have addressed the relationship between the physical or aerodynamic particle size distribution (APSD) of pharmaceutical aerosols and lung deposition. This is likely due to the need for using imaging

* Corresponding author. Tel.: +61 2 9351 3054; fax: +61 2 9351 4391.
E-mail address: kimc@pharm.usyd.edu.au (H.-K. Chan).

techniques to study lung deposition that are less readily available (Chan et al., 2006). Thus, it remains unclear just how *in vitro* dispersion performance translates to *in vivo* deposition in the lung (Newman, 1998).

The purpose of the present study was to link changes in the *in vitro* particle size of a DPI to the *in vivo* lung deposition using SPECT and mannitol as the dry powder with different particle sizes. Mannitol is a sugar alcohol, and is used as a dry powder by inhalation for diagnosis of bronchial hyperresponsiveness (Anderson et al., 1997; Brannan et al., 2005). Being an osmotic agent, mannitol is also used for enhancing clearance of mucus in people with bronchiectasis and cystic fibrosis (Daviskas et al., 1997, 1999, 2001, 2005; Robinson et al., 1999). Mannitol was primarily chosen as a model in this study because its particle size can be readily controlled by spray drying (Chew and Chan, 1999) and the spray-dried powder is crystalline and physically stable (Rowe et al., 2001).

2. Method

2.1. Human subjects

Eight human subjects (three male, five female) aged between 20 and 29 (mean \pm standard error of the mean: 22.3 ± 1.1) with height 156–180 cm (165.9 ± 3.1) were recruited for the study. All subjects were healthy, non-smokers and had a forced expiratory volume in 1 s (FEV_1) $> 98\%$ predicted (110.6 ± 3.1). All subjects had no significant reactivity to mannitol in response to inhaling increasing doses of mannitol up to 75 mg on the screening visit (% fall in FEV_1 was $< 3\%$).

The study was approved by the Ethics Committee of both the University of Sydney and the Sydney South West Area Health Service. Mannitol was used under the clinical trial notification scheme of the Therapeutic Goods Administration of Australia (CTN Trial No. 2003/49).

2.2. Preparation of radiolabelled mannitol powder

Mannitol solutions at the required concentrations (Table 1) were prepared by dissolving the raw material (mannitol 99%, Mallinckrodt, NJ, USA) in deionised water. A fresh ^{99m}Tc -

DTPA complex was prepared by adding approximately 4 GBq ^{99m}Tc -pertechnetate in normal saline to a DTPA (Radpharm, Australia) vial and made up to 2 mL with water for injection. This complex was then added to an autoclaved mannitol feed solution prior to spray drying. A spray dryer (Büchi Mini spray dryer, B-191, Switzerland) was employed to produce spray-dried particles with volume median diameters of 2, 3 and 4 μm using the operating conditions outlined in Table 1. To minimise environmental microbial contamination, the spray dryer was modified as follows: (1) the inlet air was filtered using a 0.2 μm particulate filter (Aervent Opticap XL2, Millipore, USA) and (2) the compressed air was filtered using a 0.65 μm Tuffryn membrane filter (Pall Life Sciences, East Hills, NY, USA).

For validation purposes, powders were produced without the radioactive marker ^{99m}Tc -DTPA. Bioburden analysis performed on validation samples showed that they comply with British Pharmacopoeia standards for inhalation powders (total viable aerobic count, TVAC $< 10^2$ cfu/g). Particle size was confirmed on the validation powders as well as the labelled powders using laser diffraction (Mastersizer S, Malvern, Worcs, UK). The powders (20 mg) were dispersed by sonication for 1 min in chloroform (30 mL) containing a drop (0.05 mL) of Tween 80 as the dispersion medium. A suitable amount of the suspension was then added into the dispersion cell of the equipment stirring at 2000 rpm to circulate the particles through the measuring zone while keeping the obscuration between 10 and 20%. Particle size analysis was based on the refractive index (RI) of mannitol (1.520), $RI_{imaginary}$ of mannitol (0.100) and chloroform (1.444). The particle size distribution was expressed as the volume median diameter and span (defined as the difference in particle diameters at 10 and 90% of the cumulative volume, respectively, divided by the volume median diameter). Using scanning electron microscopy (JEOL 6000 field emission SEM) all particles were found to be smooth and spherical like those in our previous study (Chew and Chan, 1999). The physical stability was confirmed by the minimal moisture sorption (0.62 wt% at 90% RH). The amount of radioactivity per gram of mannitol ranged between 1 and 1.5 GBq/g. In addition, thin layer chromatography of ^{99m}Tc -DTPA in saline prior to spraying and in the spray powders (after reconstitution in water) confirmed that the ^{99m}Tc -DTPA complex was maintained after the spray-drying process.

Table 1
Spray-drying conditions for mannitol powders and particle size data

Powder	Mannitol feed concentration (g/mL)	Feed rate (mL/min)	Atomising nozzle air flow (NL/h)	Powder ^a		Aerosol ^b	
				Volume median diameter (VMD) (μm) ^c	Span	MMAD (μm)	GSD
2 μm	0.0075	0.7	700–800	2.1 (2.0–2.2)	2.3	2.7	2.6
3 μm	0.0133	0.7	650–750	2.9 (2.8–3.0)	2.0	3.6	2.4
4 μm	0.02	1.6	400–500	4.0 (3.8–4.1)	2.1	5.4	2.7

^a This refers to the primary particle size distribution measured by laser diffraction by dispersing the powder in liquid (as described in Section 2.2).

^b This refers to the particle size distribution of the aerosol when the powder was dispersed using an Aeroliser[®]; MMAD and GSD are mass median aerodynamic diameter and geometric standard deviation, respectively. GSD was obtained from the best fit line of the aerosol size distribution, which however is not perfectly log-normal.

^c The numbers in brackets indicate the range of particle sizes for the radiolabelled powders produced ($n = 3$).

2.3. *In vitro* powder dispersion

Each of the mannitol powders (~20 mg) was loaded into a size 3 hydroxypropyl methyl cellulose (HPMC) capsule (Capsugel, NJ, USA) and was dispersed at 60 and 100 L/min using an Aeroliser® dry powder inhaler [device resistance $0.06 \text{ cmH}_2\text{O}^{1/2}/(\text{L}/\text{min})$] connected via an USP induction port to a model 160 Marple Miller Impactor (MSP Corp., MN, USA). Each run was performed in triplicates. The collecting cups were coated with silicone grease (Dow Corning, Australia) to reduce the effect of particle bounce. After each dispersion the powder collected at each stage of the impactor, induction port, capsule and device was dissolved in a known amount of deionised water. The amount of radioactivity in each sample was measured on a CRC-5 radioisotope calibrator (Capintec, Ramsey, NJ, USA). A previously validated high performance liquid chromatography (HPLC) method (Chew and Chan, 2002) enabled mannitol to be chemically assayed within an established working range of 0.025–4 mg/mL using refractive index detection. Fine particle fraction (FPF) is defined as the mass fraction of particles less than $5 \mu\text{m}$ in the aerosol, corresponding to those collected on stages 3, 4, 5 and the filter. FPF is referenced against the recovery (i.e. dose in impactor including induction port+device and capsule retention) and is expressed as the mean of triplicate runs. When altering air flow rate, the impaction stage cutoffs were re-calculated based on the inverse square root of the air flow (Feddah et al., 2000). Interpolation was used to determine the fine particle fraction under $5 \mu\text{m}$ when the dispersion flow rate differed from 60 L/min.

2.4. Administration of mannitol powder

Inhalation of the different particle size powders by the subjects occurred on separate study days. On each study day the subject practiced their inhalation technique using an Aeroliser® dry powder inhaler with empty capsules to obtain reproducible flow profiles. A 20 mg dose of non-radioactive mannitol was administered to each subject to condition the airways to mannitol in order to minimise potential coughing during the inhalation of radiolabelled mannitol. Three capsules each containing 20 mg of the radiolabelled mannitol were separately loaded into the Aeroliser® DPI and subjects were requested to inhale with maximum respiratory effort. After inhalation the subjects were instructed to hold their breath for 5 s before exhaling into a ‘Respirgard II™’ particulate filter (type 303, Vital Signs, NJ, USA). Imaging was commenced 5 min after the start of inhalation of the first capsule.

Inhalation flow profiles were recorded during inhalation of the radiolabelled powders by each subject. This was done using a flow meter (TSI model 4040 E) connected to the analogue input of an oscilloscope. Signals were saved as digital files for further data analysis. The inhalation volume was calculated using the trapezium rule as the area under the flow vs. time profile. Acceleration of flow was calculated as the slope from baseline to peak flow. The peak inhalation flow data of the subjects are summarised in Table 2.

Table 2

Peak inhalation flow data of the eight subjects who participated in the study

Subject number	Flow rate (L/min)		
	2 μm	3 μm	4 μm
1	116	121	123
2	114	111	110
3	109	109	107
4	126	132	128
5	117	123	117
6	142	135	141
7	108	104	111
8	94	95	100

2.5. SPECT imaging and data analysis

Simultaneous emission and transmission fast SPECT studies were acquired on a triple head gamma camera (Triad XLT, Trionix, USA) as previously described (Eberl et al., 2001). Two of the three detectors were fitted with high resolution parallel hole collimator for the emission measurements, while the detector opposing the transmission line source was fitted with a fan-beam collimator with a focal length of 1140 mm for transmission measurement. The transmission line was filled with approximately 1GBq of $^{99\text{m}}\text{Tc}$. A two frame, 1 min/frame dynamic SPECT study was performed at three-bed positions to cover an extended axial length including the oropharynx, lungs and abdomen with the limited axial field of view (FOV) of 23 cm of the gamma camera. Between each dynamic SPECT, the bed was moved, under computer control, to the next bed position and the image acquisition was repeated. This allowed 68 cm to be covered along the subject, with a slight overlap of bed positions. Three such passes were collected, the first two with the transmission source open, while the last one with the transmission source closed to allow estimation of the cross talk from the activity in the subject into the transmission images. A transmission blank scan was performed on each study day.

2.6. Image reconstruction and data analysis

Each set of 2×1 min frames was summed into a single frame for the emission data and the projections from each set of three-bed positions were assembled into a single volume, taking into account the bed overlap to give a projection data set covering the full length of the acquisition. The four frames of transmission data with the transmission source open were also summed into a single frame and rebinned from fan-beam to parallel data. Cross talk correction factors of emission counts contributing to transmission counts were determined from the scan with the transmission source closed. Emission images simultaneously collected with the transmission images were multiplied by the cross talk correction factors before being subtracted from the transmission data. The transmission data were corrected by the blank scan and reconstructed with OSEM (ordered subset expectation maximisation, 1 iteration, 30 subsets) (Hudson and Larkin, 1994). The emission data were

reconstructed with OSEM (2 iteration, 6 subsets) and attenuation corrected using the reconstructed transmission data. A three-dimensional Gaussian post-reconstruction filter (11 mm FWHM, full width at half maximum) was applied to reduce noise in the images.

Total activity in the subject and activity in the lungs, oropharynx and stomach and GI tract were then estimated from the first multi-bed position study using manually defined regions of interest (ROIs). The cross calibration factor to convert SPECT counts to activity concentration were determined from a phantom study containing known amounts of activity in “lung”, “stomach” and “oropharynx” compartments. The phantom studies were acquired and processed in the same way as the subject studies.

The automatically defined right lung volume of interest (Eberl et al., 2001) was divided into 10 concentric shells (Fleming et al., 1995, 1996; Eberl et al., 2001). The central region was defined as the five innermost shells, while the two outermost shells comprised the peripheral region. The remaining three shells comprised the intermediate region. The penetration index (PI) was calculated from the ratio of the counts per voxel in the peripheral region to the counts per voxel in the central region. The peripheral region includes predominantly the small airways as well as alveoli of the lung where actual oxygen-exchange occurs. Because of the thin barrier for absorption, this region is targeted for drugs with a systemic effect.

2.7. Statistical analysis

Analysis of variance (ANOVA with repeated measures) was performed to compare the dose and distribution effect of the different particles sizes of powder mannitol (Statview 5, SAS Institute, Cary, North Carolina). Probability values less than 0.05 were considered statistically significant. Results were reported as mean \pm standard error of the mean (S.E.M.) unless otherwise stated.

3. Results

3.1. Radiolabelling validation and chemical assay

Initially the spray-drying techniques used to radiolabel the mannitol powders were validated by performing *in vitro* powder dispersions and chemical assays. The chemical assay results followed the radioactivity distribution for the mannitol powders of all three-particle sizes (Fig. 1). The aerosol particle size distributions of the radiolabelled and control (non-radiolabelled) powders were also similar, indicating that the radiolabelling method did not alter the aerosol performance of the mannitol powder. The homogeneity of the radiolabel in the powder, shown by the close match of the mannitol with the radioactivity in Fig. 1, was expected since the powders were produced from solutions containing both mannitol and the radiolabel which distributed uniformly in the water. The results thus confirmed the validity of quantifying the mass of mannitol in the lung by measuring the radioactivity.

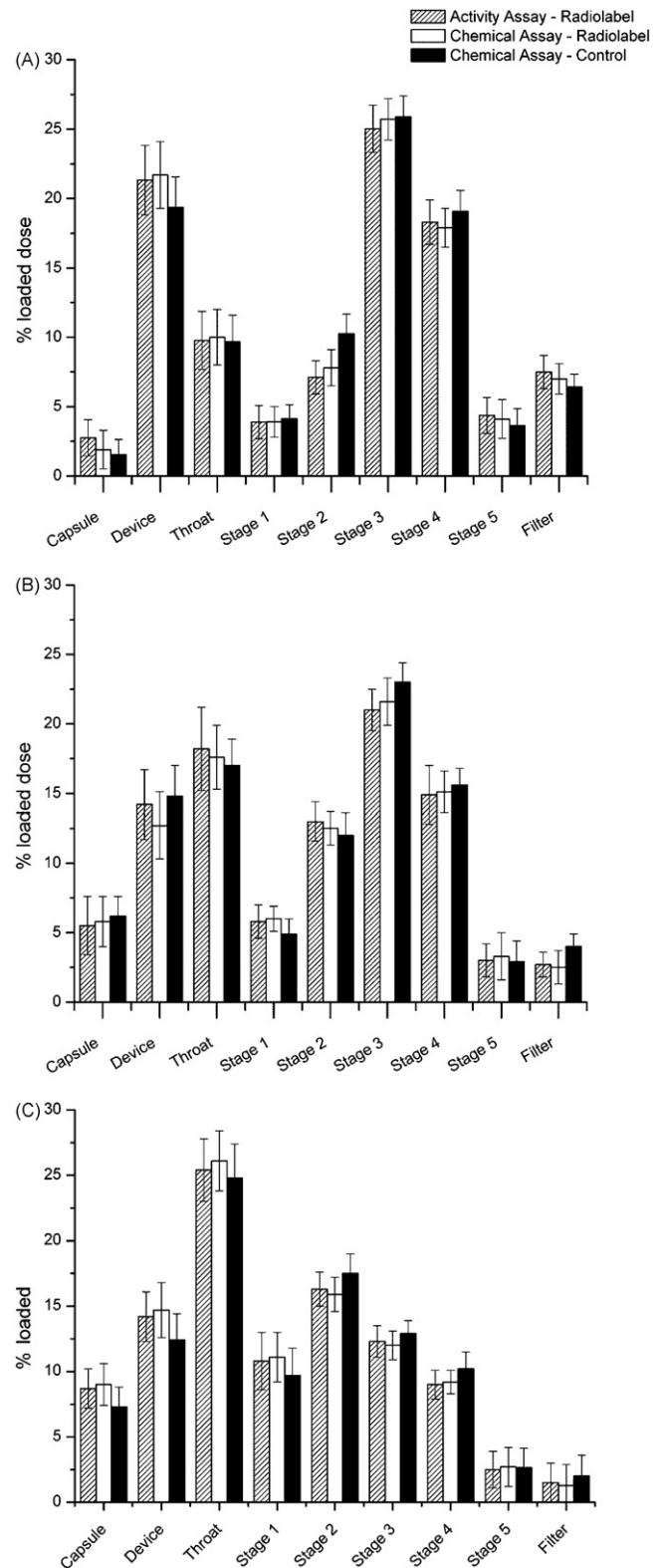


Fig. 1. Validation graphs of *in vitro* distribution of the powders as a function of impactor stage for (A) 2 μm powder, (B) 3 μm powder and (C) 4 μm powder (error bars showing standard deviation, $n = 3$). The graphs demonstrate that the activity of the radiolabelled powder (activity assay—radiolabel) and the chemical assay of the radiolabelled powder (chemical assay—radiolabel) closely follow the chemical assay of the unlabelled powder (chemical assay—control). Thus, the radiolabelling does not change the *in vitro* distribution of the powder and the radioactivity distribution can be used as a surrogate for chemical assay.

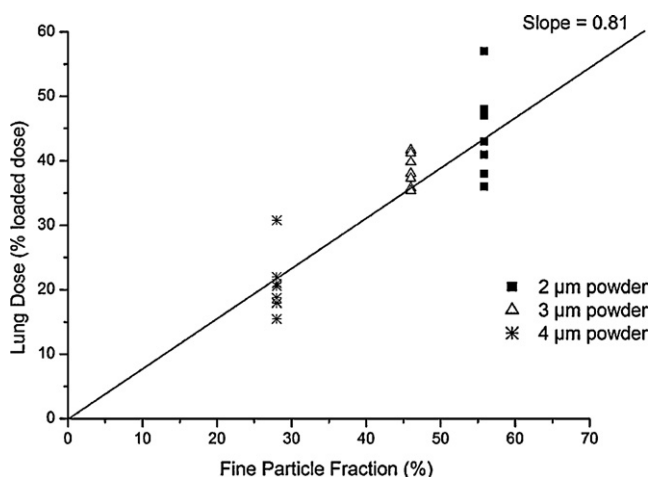


Fig. 2. Lung dose (percent of loaded dose) plotted as a function of fine particle fraction ($<5 \mu\text{m}$) for the three powders. The regression line shown (for 24 data points) has been fitted with the intercept forced through the origin to allow direct estimate of % FPF deposited in the lungs from the slope. Thus, the slope of 0.81 indicates that 81% of the FPF deposits in the lungs for these powders.

3.2. *In vitro* dispersions

The *in vitro* dispersion data generated at 60 L/min showed that the 2, 3 and 4 μm powders (with span 2.3, 2.0 and 2.1, respectively) had a fine particle fraction (FPF) under 5 μm of 55.8% (range 53–57), 46.0% (range 45–48) and 28.3% (range 26–29) of the loaded dose, respectively. While there is a strong dependence of the FPF on the particle size, FPF was not affected by the air flow between 60 and 100 L/min (55.1 ± 1.5 , 46.0 ± 1.4 , 28.1 ± 1.6 at 60L/min vs. 57.1 ± 3.0 , 49.1 ± 2.0 , 29.1 ± 1.6 at 100 L/min for the 2, 3 and 4 μm powders, respectively).

4. Mannitol deposition

4.1. Lung dose

Overall the lung dose (i.e. radioactivity in the lungs) of the dry powder mannitol, inhaled using the low resistance

DPI (Aeroliser[®]), increased as the primary particle size of the mannitol powder was decreased (Fig. 2). Fig. 3 illustrates the results showing coronal slices of SPECT images of a subject (no. 7). The mean \pm S.E.M. doses expressed as a percentage of the loaded dose were 44.7 ± 2.4 , 38.9 ± 0.9 and $20.6 \pm 1.6\%$ for the 2.7, 3.6 and 5.4 μm aerosols, respectively ($p < 0.0001$). These percentages corresponded to a range of 21.2–34, 21.2–25 and 9.2–18.5 mg of the initial 60 mg loaded dose for each particle size. The lung dose of the 5.4 μm aerosols was distinctly different from and approximately only half of that of the 2.7 and 3.6 μm aerosols ($p < 0.0001$). The difference in the lung dose between the 2.7 and 3.6 μm aerosols was significant ($p < 0.02$) but small. Further, the lung dose for each particle size was consistently lower than the *in vitro* FPF ($<5 \mu\text{m}$) of the mannitol powders. A linear regression line fitted to the data shows a slope of 0.81 ($r^2 = 0.81$, $p < 0.0001$) with the fit intercepts forced through the origin (which results in the slope providing a direct measure of % FPF deposited in the lungs), indicating that the lung dose is only 81% of the *in vitro* FPF (Fig. 2). The regression equation without forcing the intercepts through the origin is $y = 0.899x - 4.246$ ($r^2 = 0.82$, $p < 0.0001$) where y is the lung dose (as % loaded dose in the inhaler) and x is the % FPF under 5 μm .

The intersubject coefficient of variation (CV%) in the lung dose was 15.3, 6.6 and 22.5% for the 2.7, 3.6 and 5.4 μm aerosols, respectively. No dependence of the *in vivo* lung dose on the subjects inhalation flow rate (range 94–142 L/min) was found (Fig. 4).

4.2. Lung distribution

The lung distribution of mannitol was calculated from the SPECT imaging data and expressed as the penetration index (PI). Mannitol was deposited diffusely in the lung for all three-particle sizes. The 2.7 and 3.6 μm aerosols gave an average PI of 0.63 ± 0.05 (range: 0.37–0.78) and 0.60 ± 0.04 (range: 0.45–0.68), compared with 0.52 ± 0.04 (range: 0.31–0.66) for the 5.4 μm aerosols (Fig. 5). There was a significant differ-

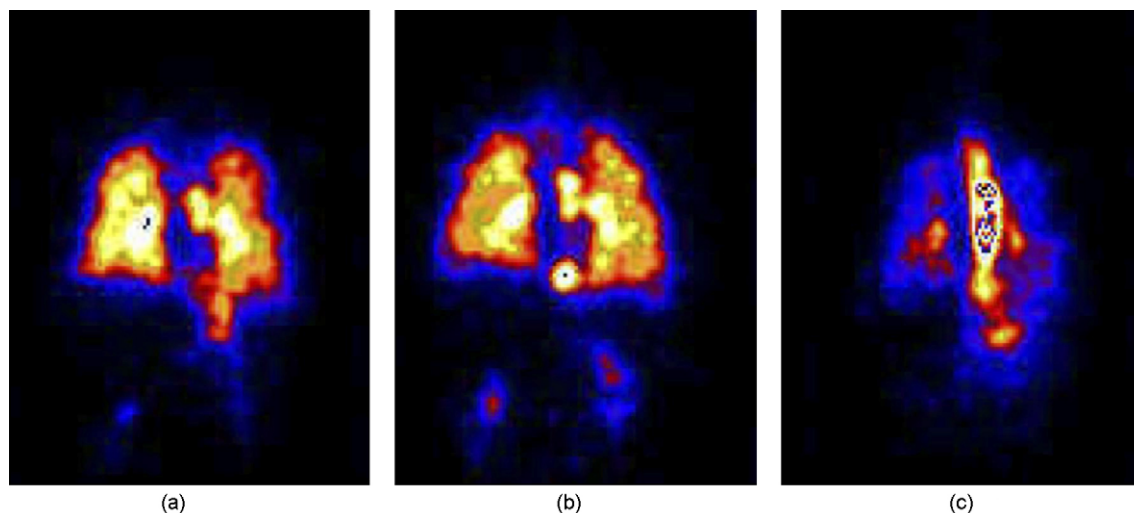


Fig. 3. Coronal slices from the SPECT images obtained after inhalation of the radiolabelled mannitol powders in one of the subjects (no. 7). (a) 2, (b) 3 and (c) 4 μm .

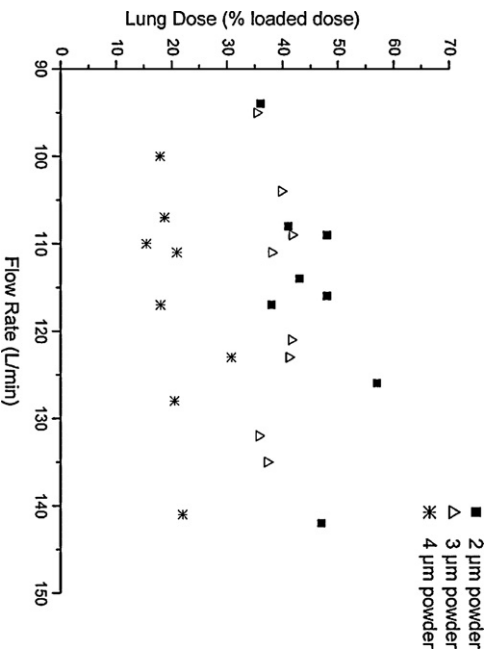


Fig. 4. Lung dose vs. peak inhalation flow rate achieved by the subjects. Over the range of inhalation flow rates achieved, there is no dependence of lung dose on the inhalation flow rate.

ence in the PI results between the 5.4 and 2.7 or 3.6 μm aerosols ($p < 0.02$), but not between the 2.7 and 3.6 μm aerosols ($p > 0.3$). The actual mass of mannitol deposited in the central and peripheral regions of the lungs is summarised in Table 3.

4.3. Extrathoracic deposition

The amounts of the mannitol powder deposited in the oropharynx and gastro-intestinal tract were combined as an indicator of throat deposition. On average $75.9 \pm 2.2\%$ of the 5.4 μm aerosol deposited in the upper airways, compared with 42.4 ± 2.4 and $36.0 \pm 2.5\%$ for the 3.6 and 2.7 μm aerosols, respectively ($p < 0.0001$) (Fig. 6). The difference in the upper airways deposition between the 2.7 and 3.6 μm aerosols was also significant ($p < 0.05$) but of smaller magnitude. Only minimal amounts of all sizes of the mannitol powders were exhaled as

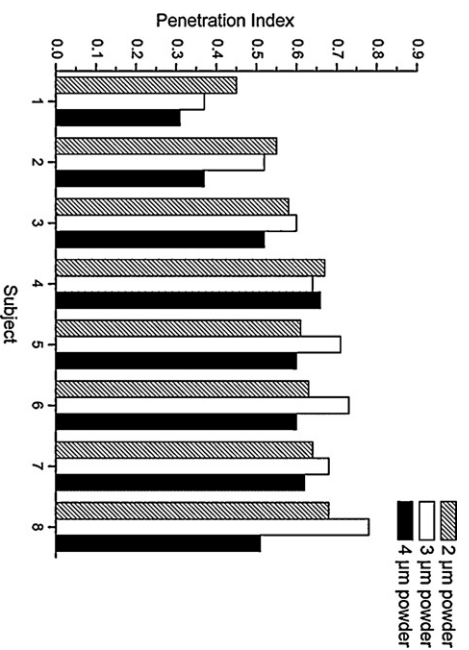


Fig. 5. Penetration indices for the subjects as a function of particle size. The penetration indices of the 2 and 3 μm powders (VMD) (MMAD 2.7 and 3.6 μm, respectively) were significantly higher than those of the 4 μm (VMD) (MMAD 5.4 μm) powder. However, there was no significant difference between the penetration indices of the 2 and 3 μm powders.

Table 3
Mass (mg) of mannitol deposited in the central, intermediate and peripheral regions of the right lung for a 60 mg loaded dose of powder based on radioactivity

Subject	Mass of powder deposited in the lungs (mg)								
	2 μm			3 μm			4 μm		
	Central	Intermediate	Peripheral	Central	Intermediate	Peripheral	Central	Intermediate	Peripheral
1	4.8 (0.019)	8.2 (0.012)	4.1 (0.008)	4.8 (0.021)	6.9 (0.011)	3.6 (0.008)	3.3 (0.025)	4.8 (0.011)	2.7 (0.008)
2	2.7 (0.028)	6.8 (0.023)	4.4 (0.017)	2.8 (0.026)	6.1 (0.021)	4.0 (0.016)	1.4 (0.013)	2.3 (0.007)	1.3 (0.005)
3	3.4 (0.025)	7.4 (0.019)	4.6 (0.015)	2.9 (0.024)	6.9 (0.020)	4.6 (0.016)	1.4 (0.010)	2.9 (0.007)	1.8 (0.005)
4	3.7 (0.029)	8.1 (0.023)	5.1 (0.018)	2.7 (0.022)	5.6 (0.017)	3.7 (0.014)	1.5 (0.013)	3.4 (0.010)	2.1 (0.009)
5	2.5 (0.016)	5.6 (0.013)	2.9 (0.009)	2.8 (0.021)	6.3 (0.017)	3.6 (0.012)	2.3 (0.022)	5.1 (0.017)	3.3 (0.013)
6	3.4 (0.016)	8.3 (0.013)	4.3 (0.009)	2.9 (0.010)	6.2 (0.008)	3.2 (0.006)	1.7 (0.010)	3.4 (0.008)	2.3 (0.006)
7	2.5 (0.024)	6.4 (0.024)	3.8 (0.017)	2.9 (0.040)	6.0 (0.032)	4.0 (0.025)	1.4 (0.023)	3.4 (0.019)	2.2 (0.014)
8	2.3 (0.022)	5.2 (0.019)	3.6 (0.016)	2.0 (0.019)	5.2 (0.018)	4.0 (0.016)	1.4 (0.013)	2.7 (0.009)	1.7 (0.007)
Mean ± S.E.M.	3.2 ± 0.3 (0.022 ± 0.002)	7.0 ± 0.4 (0.018 ± 0.002)	4.1 ± 0.2 (0.014 ± 0.002)	3.0 ± 0.3 (0.023 ± 0.003)	6.1 ± 0.2 (0.018 ± 0.002)	3.8 ± 0.1 (0.014 ± 0.002)	1.8 ± 0.2 (0.016 ± 0.002)	3.5 ± 0.3 (0.011 ± 0.002)	2.2 ± 0.2 (0.008 ± 0.001)

Data in parentheses represent the mass of mannitol per volume (mg/mL) of the lung regions.

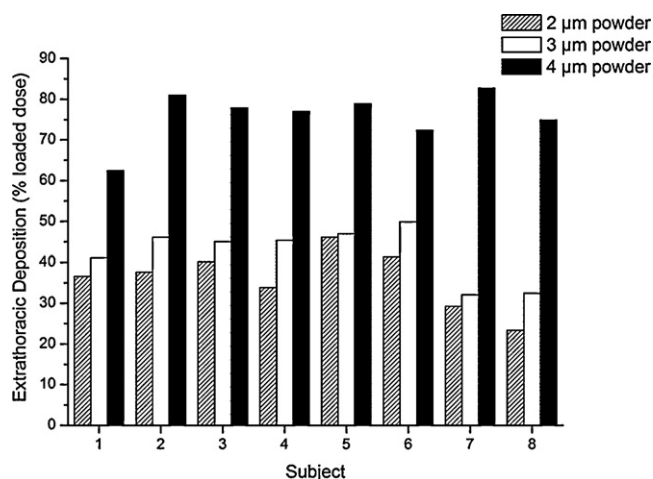


Fig. 6. Percent throat deposition as a function of particle size for the subjects. Throat deposition with the 4 µm powder (VMD) (MMAD 5.4 µm) was almost twice the deposition observed with the smaller particle size powders. A small, but significant reduction in throat deposition is also observed with the 2 µm powder (VMD) (MMAD 2.7 µm) when compared with the 3 µm powder (VMD) (MMAD 3.6 µm).

indicated by the low levels (less than 0.5%) of activity detected in the exhalation filter.

5. Discussion

Mannitol powders with primary particle size 2.1, 2.9 and 4.0 µm (VMD) and similar polydispersity (span: 2.3, 2.0 and 2.1 respectively), corresponding to 2.7, 3.6 and 5.4 µm MMAD (GSD: 2.5, 2.2 and 2.7 respectively), when dispersed by the dry powder inhaler Aeroliser[®] were used in the study. The unimodal size distributions with a similar polydispersity, but different only in the median particle size for the powders made it feasible to use the median size for comparing the deposition behaviour. Different polydispersities would have affected the contact area (hence cohesion) between particles and confounded the comparison (Fuchs, 1964).

The key findings of the study are (i) the aerosol dose in the lungs increased as the aerosol particle size decreased from 5.4 to 2.7 µm; (ii) the distribution of the mannitol within the lungs measured by the penetration index was similar between the 2.7 and 3.6 µm aerosols but different to the 5.4 µm aerosol. Thus, both the dose and distribution of the aerosol within the lung depend on the particle size of the powder used. The throat deposition in the subjects was also dependent on the particle size, with the throat deposition of the 5.4 µm aerosol being roughly double of the values for the 2.7 and 3.6 µm aerosols. These results were obtained using pure mannitol powders without any lactose carrier, hence the findings may not necessarily be applicable to blend formulations containing more than one component.

Full characterisation of aerosol deposition not only in the lungs but also in extra thoracic areas such as the oropharynx and stomach requires the ability to estimate activities in diverse regions with heterogeneous attenuation. This mandates transmission based attenuation correction and the diverse regions pose a considerable challenge to accurate estimation of activ-

ity with planar imaging. The fast dynamic SPECT imaging previously implemented (Eberl et al., 2001) was adapted to cover the required axial extent in a sufficiently short time to avoid appreciable redistribution of activity over the duration of the study. Absolute activity quantitation from the SPECT data allows “mass” or activity balance calculations to be performed. The total recovery of radioactivity calculated from the total activity in the subject estimated from the SPECT study plus the residual left in the capsule and inhalation device for each subject was in the range of 90–100% of the loaded dose (data not shown). This provides confirmation and reassurance that an accuracy of around 10% is achieved with the SPECT aerosol activity distribution estimates.

The increase in lung dose with the smaller particles was consistent with the *in vitro* dispersions of the mannitol powders which showed a significant increase in FPF as the primary particle size of the powder was decreased. The present *in vitro*–*in vivo* correlation with a slope of 0.81 provides a reasonable predictor of lung deposition from the FPF. The over-estimation of lung dose by the FPF data was commonly found in MDI and DPI studies, and is due to the inadequacy of using a single particle cutoff to account for the complex deposition of aerosol particles in the lungs (Clark and Borgstrom, 2002). The present slope value of 0.81 is consistent with earlier results using the Cyclohaler[™] DPI coupled with a human cast throat (Olsson et al., 1996). The variation of the lung dose between subjects in the present study was low (CV = 7–23%) and compares favourably with other studies performed using other inhalers where of the CV was between 14 and 49% (Pitcairn et al., 2000). It has been reported that the inhaler resistance would affect the geometry of the upper airway (hence aerosol deposition) during inhalation (Mcrobbie and Pritchard, 2005). It is worth noting that when the 3 µm powder was dispersed from the high resistance inhaler, Inhalator[™] (Glover et al., 2006), the lung dose was much lower (24.7 ± 5.2%) compared with 38.9 ± 0.9% in the present study. The difference in the results can readily be attributed to the different FPF, MMAD, air flow rates and device resistance (Inhalator[™]: 25–42%, 4.1 µm, 43–63 L/min and 0.18 cmH₂O^{1/2}/(L/min) vs. Aeroliser: 45%, 3.6 µm, 95–140 L/min and 0.06 cmH₂O^{1/2}/(L/min)) (Clark and Hollingworth, 1993; Glover et al., 2006). The results thus highlight the important role of the inhaler device in deposition of DPI aerosols in the lungs.

The influence of individual subject flow patterns was investigated to see if it could explain the inter-subject variation in lung dose. No dependence of the *in vivo* lung deposition on the subject’s inhalation flow rate was found, although the deposition of the 2 µm powder appeared to be more variable. This is in contrast with the earlier findings using the 3 µm mannitol powder dispersed with the high resistance DPI, Inhalator[™], where the lung dose was increased with higher peak inhalation flows (which produced a higher FPF) (Glover et al., 2006). A slight, but significant correlation between the inhalation flow and deposition was previously seen for the deposition of eformoterol using the Aeroliser[®] (Meyer et al., 2004). However, a much larger flow range of 30–130 L/min with lower flow rates was employed in that study. The lack of a definite trend in lung

deposition vs. inhalation flow rate can be partially explained by the *in vitro* dispersion data, which showed no difference in the FPF between 60 and 100 L/min indicating that a maximum FPF occurs at ≥ 60 L/min. We attribute this to the critical turbulence concept introduced by Coates et al using the Aeroliser® DPI, i.e. the fine particle fraction will plateau once a critical level of turbulence is generated within the device (Coates et al., 2005).

The distribution of the deposited aerosols in the lung follows the expectation that smaller particles deposit more peripherally than larger particles, as reflected by an increase in the PI values as the aerosol particle size is reduced from 5.4 to 2.7 μm . The clinical relevance of these findings is that increased lung doses can be achieved using powders of smaller particle size. It is generally believed that powders with larger particle size deposit more centrally which could be more suitable for targeting the large airways. Our results showed that smaller particles can actually give a higher dose (both absolute mass and mass per lung volume) in all regions of the lungs (Table 3). The results do not support the use of mannitol powder of primary particle size greater than 3 μm as clinically suitable, since 76% of the loaded dose of 4 μm diameter particles was deposited in the throat. In contrast, effective doses of powders of mannitol of 3 μm or less could be delivered for clinical use and their success is supported by multiple studies (Anderson et al., 1997; Daviskas et al., 1997, 1999, 2001; Robinson et al., 1999; Brannan et al., 2005). However, it is essential to ensure that the powder can be sufficiently dispersed *in vitro* when a smaller particle size such as 2 μm is chosen as the powder will become more cohesive with reduced particle size. Particle size reduction will increase the specific surface area of the powder, and since the particles of the three powders were spherical with smooth surface morphology, size reduction is thus likely to increase contact area and cohesion between particles. Furthermore, since mannitol is crystalline and non-hygroscopic, the results may not necessarily be directly applicable to powders which are amorphous and/or undergo hygroscopic growth in the airways. The present results on powders of pure mannitol as drug also would have limited applicability for binary mixtures involving both drug and carrier.

Finally, it is worth to consider a potential implication of the results on the formulation and manufacturing of DPI products. While the reduction of the aerosol MMAD from 5.4 to 3.6 μm improves the lung dose significantly, further aerosol particle size reduction from 3.6 to 2.7 μm has only a marginal improvement. Due to the low collection efficiency of the cyclone, the yield of the 2 μm powder by spray drying is quite poor (30%). If mechanical milling were employed instead of spray drying, it would have been highly energy demanding to reduce the 3 μm powder further down to 2 μm , accompanied by amorphous materials generated during the processing. Either way, it is not cost-effective, hence it would not be worth the extra effort to produce a DPI product with the smaller 2.7 μm aerosols unless the marginal improvement of the lung dose can be justified by positive clinical outcomes in terms of efficacy and unwanted side effects. The situation may be different for a higher resistance inhaler with the same dispersion efficiency (i.e. same FPF) as

the lower inhalation air flow is likely to reduce the extrathoracic deposition and hence increase the lung dose.

6. Conclusion

In conclusion, SPECT has been used to establish the particle size dependence of *in vivo* lung deposition of mannitol aerosols. The dose delivered to the lung with the 2.7 and 3.6 μm aerosols was double compared to the dose with the 5.4 μm aerosol delivered using the low resistance device Aeroliser®. This increase in lung dose also follows the increase in cascade impactor-measured aerosol performance with decreasing particle size. Deposition of the inhaled powder was increased in the lung periphery as the particle size was decreased. The results indicate that both the dose and site of deposition of dry powder mannitol aerosols within the lung depend significantly on the particle size of the powder dispersed with the low resistance DPI Aeroliser®. The findings of the present study may apply to other powders that are pure, stable, crystalline and polydisperse when dispersed with a low resistance DPI.

Acknowledgements

The authors would like to thank the following: Dr. Sandra Anderson for her valuable suggestions to the manuscript, Drs. Iven Young and Michael J. Fulham for their supports, all of the volunteers who participated in this study, the University of Sydney for the Sesqui Research Grant and the Australian Research Council for funding the scholarship held by W. Glover.

References

- Anderson, S.D., Brannan, J., Spring, J., Spalding, N., Rodwell, L.T., Chan, H.-K., Gonda, I., Walsh, A., Clark, A.R., 1997. A new method for bronchial provocation testing in asthmatic subjects using a dry powder of mannitol. *Am. J. Respir. Crit. Care Med.* 156, 758–765.
- Ball, D., Hirst, P., Newman, S., Bernard, S., Streeb, B., Vanderbist, F., 2002. Deposition and pharmacokinetics of budesonide from the Miat monodose inhaler, a simple dry powder device. *Int. J. Pharm.* 245, 123–132.
- Brannan, J., Anderson, S.D., Perry, C.P., Freed-Martens, R., Lassig, A.R., Charlton, B., 2005. The safety and efficacy of inhaled dry powder mannitol as a bronchial provocation test for airway hyperresponsiveness: a phase 3 comparison study with hypertonic (4.5%) saline. *Respir. Res.* 6, 144.
- Chan, H.-K., Eberl, S., Glover, W., 2006. Radiolabelling of pharmaceutical aerosols & gamma scintigraphic imaging for lung deposition. In: *Encyclopedia of Pharmaceutical Technology*. Merck Dekker, New York.
- Chew, N.Y.K., Bagster, D.F., Chan, H.K., 2000. Effect of particle size, air flow and inhaler device on the aerosolisation of disodium cromoglycate powders. *Int. J. Pharm.* 206, 75–83.
- Chew, N.Y.K., Chan, H.-K., 1999. Influence of particle size, air flow, and inhaler device on the dispersion of mannitol powders as aerosols. *Pharm. Res.* 16, 1098–1103.
- Chew, N.Y.K., Chan, H.-K., 2002. Effect of powder polydispersity on aerosol generation. *J. Pharm. Pharm. Sci.* 5, 162–168.
- Clark, A., Borgstrom, L., 2002. In vitro testing of pharmaceutical aerosols and predicting lung deposition from in vitro measurements. In: Bisgaard, H., O'callaghan, C., Smalldone, G.C. (Eds.), *Drug Delivery to the Lung*. Merck Dekker, New York.
- Clark, A., Hollingworth, A., 1993. The relationship between powder inhaler resistance and peak inspiratory conditions in healthy volunteers—implications for in vitro testing. *J. Aerosol Med.* 6, 99–110.

- Coates, M., Fletcher, D., Chan, H.K., Raper, J., 2005. Influence of air flow on the performance of a dry powder inhaler using computational and experimental analyses. *Pharm. Res.* 22, 1445–1453.
- Daviskas, E., Anderson, S.D., Brannan, J.D., Eberl, S., Chan, H.K., Bautovich, G., 1997. Inhalation of dry-powder mannitol increases mucociliary clearance. *Eur. Respir. J.* 10, 2449–2454.
- Daviskas, E., Anderson, S.D., Eberl, S., Chan, H.-K., Bautovich, G., 1999. Inhalation of dry powder mannitol improves clearance of mucus in patients with bronchiectasis. *Am. J. Respir. Crit. Care Med.* 159, 1843–1848.
- Daviskas, E., Anderson, S.D., Eberl, S., Chan, H.-K., Young, I., 2001. The 24-h effect of mannitol on the clearance of mucus in patients with bronchiectasis. *Chest* 119, 414–421.
- Daviskas, E., Anderson, S.D., Gomes, K., Briffa, P., Cochrane, B., Chan, H.-K., Bautovich, G., 2005. Inhaled mannitol for the treatment of mucociliary dysfunction in patients with bronchiectasis—Effect on lung function. Health status and sputum. *Respirology* 10, 46–56.
- Eberl, S., Chan, H.-K., Daviskas, E., Constable, C., Young, I.H., 2001. Aerosol deposition and clearance measurement: a novel technique using dynamic SPECT. *Eur. J. Nucl. Med* 28, 1365–1372.
- Feddah, M.R., Brown, K.F., Gipps, E.M., Davies, N.M., 2000. In vitro characterisation of metered-dose inhalers versus dry powder inhaler Glucocorticoid products: influence of inspiratory flow rates. *J. Pharm. Pharm. Sci.* 3, 317–324.
- Fleming, J.S., Halson, P., Conway, J., Moore, E., Nassim, M.A., Hashish, A.H., Bailey, A.G., Holgate, S.T., Martonen, T.B., 1996. Three-dimensional description of pulmonary deposition of inhaled aerosol using data from multimodality imaging. *J. Nucl. Med.* 37, 873–877.
- Fleming, J.S., Nassim, M.A., Hashish, A.H., Bailey, A.G., Conway, J., Holgate, S., Halson, P., Moore, E., Martonen, T.B., 1995. Description of pulmonary deposition of radiolabeled aerosol by airway generation using a conceptual three dimensional model of lung morphology. *J. Aerosol Med.* 8, 341–356.
- Fuchs, N.A., 1964. *The Mechanics of Aerosols*. Pergamon Press, New York.
- Glover, W., Chan, H.-K., Eberl, S., Daviskas, E., Anderson, S., 2006. Lung deposition of mannitol powder aerosol in healthy subjects. *J. Aerosol Med.* 19, 522–532.
- Hudson, H., Larkin, R., 1994. Accelerated image reconstruction using ordered subsets of projection data. *IEEE T. Med. Imaging* 13, 601–609.
- Louey, M., Van Oort, M., Hickey, A., 2004. Aerosol dispersion of respirable particles in narrow size distributions produced by jet milling and spray drying techniques. *Pharm. Res.* 21, 1200–1206.
- McRobbie, D.W., Pritchard, S.E., 2005. Studies of the human oropharyngeal airspaces using magnetic resonance imaging. III. The effects of device resistance with forced maneuver and tidal breathing on upper airway geometry. *J. Aerosol Med.* 18, 325–336.
- Meyer, T., Brand, P., Ehlich, H., Kobrich, R., Meyer, G., Riedinger, F., Sommerer, K., Weuthen, T., Scheuch, G., 2004. Deposition of Foradil P in human lungs: comparison of in vitro and in vivo data. *J. Aerosol Med.* 17, 43–49.
- Newman, S.P., 1998. How well do in vitro particle size measurements predict drug delivery in vivo? *J. Aerosol Med.* 11, S97–S104.
- Newman, S.P., Hollingworth, A., Clark, A.R., 1994. Effect of different modes of inhalation on the drug delivery from a dry powder inhaler. *Int. J. Pharm.* 102, 127–132.
- Olsson, B., Borgstrom, L., Asking, L., Bondesson, E., 1996. Effect of inlet throat on the correlation between measured fine particle dose and lung deposition. In: Dalby, R., Byron, P., Farr, S. (Eds.), *Respiratory Drug delivery V*. Interpharm Press Inc..
- Pitcairn, G.R., Laninen, T., Seppala, O.-P., Newman, S.P., 2000. Pulmonary drug delivery from the taifun dry powder inhaler is relatively independent of the patients inspiratory effort. *J. Aerosol Med.* 13, 97–104.
- Robinson, M., Daviskas, E., Eberl, S., Baker, J., Chan, H.-K., Anderson, S.D., Bye, P.T., 1999. The effect of inhaled mannitol on bronchial mucus clearance in cystic fibrosis patients: a pilot study. *Eur. Respir. J.* 14, 678–685.
- Rohatagi, S., Chapel, S., Kirkesseli, S., Newman, S.P., Zhang, J., Paccaly, D., Randall, L., Wray, H., Wellington, S., Shah, B., Jensen, B.K., 2004. Pharmacoscintigraphic comparison of HMR 1031, a VLA-4 antagonist, in healthy volunteers following delivery via a nebulizer and a dry powder inhaler. *Am. J. Ther.* 11, 103–113.
- Rowe, R.C., Sheskey, P.J., Weller, P.J. (Eds.), 2001. *Pharmaceutical Excipients*. Pharmaceutical Press, London.
- Thorsson, L., Kenyon, C., Newman, S.P., Borgstrom, L., 1998. Lung deposition of budesonide in asthmatics: a comparison of different formulations. *Int. J. Pharm.* 168, 119–127.
- Zanen, P., Go, L.T., Lammers, J.-W.J., 1994. The optimal particle size for b-adrenergic aerosols in mild asthmatics. *Int. J. Pharm.* 107, 211–217.
- Zanen, P., Go, L.T., Lammers, J.-W.J., 1995. The optimal particle size for parasympatholytic aerosols in mild asthmatics. *Int. J. Pharm.* 114, 111–115.
- Zimon, A.D., 1969. *Adhesion of Dust and Powder*. Plenum Press, New York.